Clim Dyn
DOI 10.1007/s00382-009-0613-9

Multiyear simulation of the African climate using a regional climate model (RegCM3) with the high resolution ERA-interim reanalysis

Mouhamadou Bamba Sylla · E. Coppola · L. Mariotti · F. Giorgi · P. M. Ruti · A. Dell'Aquila · X. Bi

Received: 2 February 2009 / Accepted: 16 June 2009

Abstract This study examines the ability of the latest version of the International Centre for Theoretical Physics (ICTP) regional climate model (RegCM3) to reproduce seasonal mean climatologies, annual cycle and interannual variability over the entire African continent and different climate subregions. The new European Center for Medium Range Weather Forecast (ECMWF) ERA-interim reanalysis is used to provide initial and lateral boundary conditions for the RegCM3 simulation. Seasonal mean values of zonal wind profile, temperature, precipitation and associated low level circulations are shown to be realistically simulated, although the regional model still shows some deficiencies. The West Africa monsoon flow is somewhat overestimated and the Africa Easterly Jet (AEJ) core intensity is underestimated. Despite these biases, there is a marked improvement in these simulated model variables compared to previous applications of this model over Africa. The mean annual cycle of precipitation, including single and multiple rainy seasons, is well captured over most African subregions, in some cases even improving the quality of the ERA-interim reanalysis. Similarly, the observed precipitation interannual variability is well reproduced by the regional model over most regions, mostly following, and sometimes improving, the quality of the ERA-interim reanalysis. It is assessed that the performance of this model over the entire African domain is of sufficient quality for application to the study of climate change and climate variability over the African continent.

Keywords Regional climate modeling · Entire continental African domain · Low biased reanalysis · Model performance

This paper is a contribution to the special issue on West African Climate, consisting of papers from the African Multidisciplinary Monsoon Analysis (AMMA) and West African Monsoon Modeling and Evaluation (WAMME) projects, and coordinated by Y. Xue and P. M. Ruti.

M. B. Sylla (✉)
Laboratory for Atmospheric Physics, Simeon Fongang (LPASF), Polytechnic School, Cheikh Anta Diop University, BP 5085, Dakar-Fann, Dakar, Senegal
e-mail: syllabamba@yahoo.fr; msylla@ictp.it

E. Coppola · L. Mariotti · F. Giorgi · X. Bi
Physics of Weather and Climate Group, Earth System Physics Section, International Centre for Theoretical Physics (ICTP), Trieste, Italy

L. Mariotti
Department of Physics, Centre of Excellence CETEMPS, University of L'Aquila, L'Aquila, Italy

P. M. Ruti · A. Dell'Aquila
Ente per le Nuove Technologie, l'Energia e l'Ambiente (ENEA), Climate Section, Casaccia Center, Rome, Italy

1 Introduction

Regional climate models (RCMs) have been widely used as dynamical downscaling tools to study regional climate processes (e.g. Pal and Eltahir 2003; Jenkins et al. 2005; Gao et al. 2007; Abiodun et al. 2007), regional climate change (e.g. Giorgi et al. 2004b; Diffenbaugh et al. 2005; Im et al. 2007, 2008) and seasonal climate variability (e.g. Rauscher et al. 2006; Seth et al. 2006). While numerous studies have focused on the mid-latitudes (Giorgi et al. 1994; Mearns et al. 1995; Leung et al. 2004; Pal et al. 2004), relatively few have investigated the African continent (e.g. Gallée et al. 2004; Afiesimama et al. 2006; Anyah and Semazzi 2007; Segele et al. 2008; Druyan et al. 2008).

Africa is characterized by complex topographical variations and marked gradients of vegetation and land cover. It extends from the Atlantic to the Indian Ocean and from about 35°S to 35°N across the equator. Such diversity can significantly affect synoptic-scale atmospheric dynamics and oceanic boundary forcings on climate (Mutemi et al. 2007). Africa is mostly covered by semi-arid regions known for their unreliable rainfall which has a large impact on water resources and food security. The spatial climate variability is mainly associated with the occurrence of mesoscale convective systems and with the forcing of mountain complexes. The temporal variability may be seen as a modulation of the seasonal cycle linked to the meridional displacement of the rainbelt associated with the Intertropical Convergence Zone (ITCZ) and the African monsoon.

Before applying an RCM to climate variability or climate change studies for a given region, the accuracy of the model to successfully reproduce the observed regional climate characteristics should be assessed. The model performance needs to be evaluated in order to establish the model strengths and weaknesses for each region and this can be best achieved by using reanalyses of observations as lateral boundary conditions (Giorgi and Mearns 1999). In fact, several studies have demonstrated the capability of RCMs to represent details of regional climate when such models are driven by reanalysis or global climate model (GCM) output (Giorgi et al. 1993a, b; Leung et al. 2004; Sylla et al. 2009).

To date the NCEP, ERA-15 and ERA-40 reanalysis have been downscaled over Africa. For example, Afiesimama et al. (2006) and Anyah and Semazzi (2007) used RegCM3 to downscale the NCEP reanalysis, respectively, over West and East Africa. Gallée et al. (2004) used ERA-15 to drive MAR (Modele Atmospherique Regional) over West Africa. Hudson and Jones (2002) and Tadross et al. (2006) used MM5 and PRECIS to downscale ERA-15 over South Africa. Pal et al. (2007) used ERA-40 to drive RegCM3 over the entire African domain. However, these reanalysis products exhibit significant biases over the African region (Trenberth et al. 2001; Diongue et al. 2002; Tadross et al. 2006), and errors introduced by the reanalysis large-scale boundary conditions are transmitted to the RCM (Noguer et al. 1998; Giorgi and Mearns 1999; Wang et al. 2004). This adds an element of uncertainty in the evaluation of the model performance and therefore the use of "unbiased" or relatively low biased reanalysis as initial and boundary conditions in RCMs may lead to a more robust assessment of the model behaviour. Moreover, among up-to-date regional climate studies completed over Africa, only Pal et al. (2007) covered the entire African region. Because of the complex interplay among the different circulation systems affecting African climates it may be important to use large domains encompassing the entire continent.

Based on these considerations, we present here an analysis of the performance of a regional climate model (an updated version of the RegCM3 of Pal et al. 2007) driven at the lateral boundaries by the third generation of the ECMWF reanalysis, ERA-interim (Simmons et al. 2007; Uppala et al. 2008) over a large domain encompassing the entire African continent. The ERA-interim reanalysis corrects some of the errors of the ERA-40 reanalysis, particularly in the hydrologic cycle variables over the tropics (Uppala et al. 2008), and therefore probably represents the most accurate (albeit still imperfect) product available to drive an RCM over the region. In this paper we focus on different statistics (mean climatology, annual cycle and interannual variability) of relevant features of African climate, including key circulation systems, surface air temperature and precipitation, over different areas of the domain. In forth-coming papers we will focus on shorter temporal scales, from intraseasonal to daily.

2 Model description

The latest version of the ICTP regional climate model, RegCM3 (Giorgi et al. 1993a, b; Pal et al. 2007) is used in this study. RegCM3 is a primitive equation, sigma vertical coordinate, regional climate model based on the hydrostatic version of the dynamical core of the NCAR/PSU's mesoscale meteorological model MM5 (Grell et al. 1994). Radiation is represented by the CCM3 parameterization of Kiehl et al. (1996) and the planetary boundary scheme is represented by the scheme of Holtslag et al. (1990) in the implementation of Giorgi et al. (1993a). Interactions between the land surface and the atmosphere are described using the biosphere atmosphere transfer scheme (BATS1E; Dickinson et al. 1993). The scheme of Zeng et al. (1998) is used to represent fluxes from water surfaces. In RegCM3, convective precipitation can be represented by a number of schemes and here we use that of Grell et al. (1994) with the Fritsch and Chappell (1980) closure assumption. This choice was based on an analysis of the model performance in some preliminary tests. Resolvable scale precipitation processes are treated using the sub-grid explicit moisture scheme of Pal et al. (2000), which is a physically based parameterization including sub-grid scale clouds, cloud water accretion, and evaporation of falling raindrops. The model has been calibrated by modifying some key parameters, among them, the Albedo and the Stomatal Resistance.

3 Forcing and simulation design

As mentioned, the initial and lateral boundary conditions for the RegCM3 simulation are obtained from the new ERA-interim 0.75° × 0.75° gridded reanalysis (Simmons et al. 2007; Uppala et al. 2008), which is the third generation ECMWF reanalysis product. The main advances in this reanalysis compared to ERA-40 are that ERA-interim is carried out with a higher horizontal resolution with four-dimensional variational analysis, a better formulation of background error constraint, a new humidity analysis, an improved model physics, a variational bias correction of satellite radiance data and an improved fast radiative transfer model. ERA-interim uses mostly the sets of observations acquired for ERA-40 with a few exceptions: acquisition of a new altimeter wave-height that provides data of more uniform quality, use of reprocessed Meteosat data for wind and clear-sky radiance, and new ozone profile information from 1995 onwards.

Several problems experienced in the ERA-40 reanalysis have been eliminated or significantly improved in the ERA-interim. In particular, an important improvement was seen in the humidity and hydrologic cycle over the tropics. The quality of the analysis was also validated by additional means: fit of background forecasts to the observations, fit of surface winds to independent buoy winds, agreement with independent tropical-cyclone track data and comparison of precipitation with independent estimates from the Global Precipitation Climatology Project (GPCP). All pointed to a small but systematic edge in favor of the four-dimensional variational reanalysis with the variational bias correction (Uppala et al. 2008). The ERA-interim boundary conditions are updated four times daily in RegCM3.

The regional model is integrated over the continental African domain of Fig. 1 continuously for the entire 17 years period available from ERA-interim, January 1989 through December 2005, at a spatial resolution of 50 km. The domain exhibits complex and high terrains (more than 1,500 m) especially in the southern and eastern regions. Some localized highlands are also present around Cameroun (Cameroun Mountain), Central Nigeria (Jos Plateau) and Guinea (Guinea Highlands). Although a grid spacing of 50 km may still be too coarse to represent the dynamics of mesoscale convective systems as well as some local topographical features, given the large size of the domain, we decided to use this spatial resolution for initial model testing. Also shown in Fig. 1 are eight the different climate subregions selected for more detailed analysis (see below). These regions were selected in order to be broadly representative of different African climate regimes by still retaining a regular shape. It should be stressed, however, that over some areas characterized by sharp climatic gradients they may not be entirely homogeneous. For example, Indeje et al. (2000) defined eight homogeneous climate sub-regions over East Africa, which is characterized by complex topographical regions, using both EOF and simple correlation techniques.

Simulations are compared to available observation datasets such as GPCP (Global Precipitation Climatology Project; Adler et al. 2003), CRU (Climate Research Unit; Mitchell et al. 2004), FEWS (famine early warning systems; Herman et al. 1997) and to the driving ERA-interim reanalysis (ERAIM). In particular, our analysis is designed to determine whether the use of the entire continental African domain is suitable for running our regional model and if the use of the high resolution new ERA-interim reanalysis for boundary conditions may provide a more appropriate dataset for model testing and validation. In this regard, note that the lateral buffer zone is 15 grid points in size, with use of the exponential relaxation scheme of Giorgi et al. (1993b), i.e. it is small compared to the full size of the domain (220 grid points in latitude and 256 grid points in longitude). As a result, the boundary forcing, although still important, is relatively weak in the central regions of the domain. Therefore this simulation provides a stringent framework to evaluate the model's capability to represent the main African circulation and climate features.

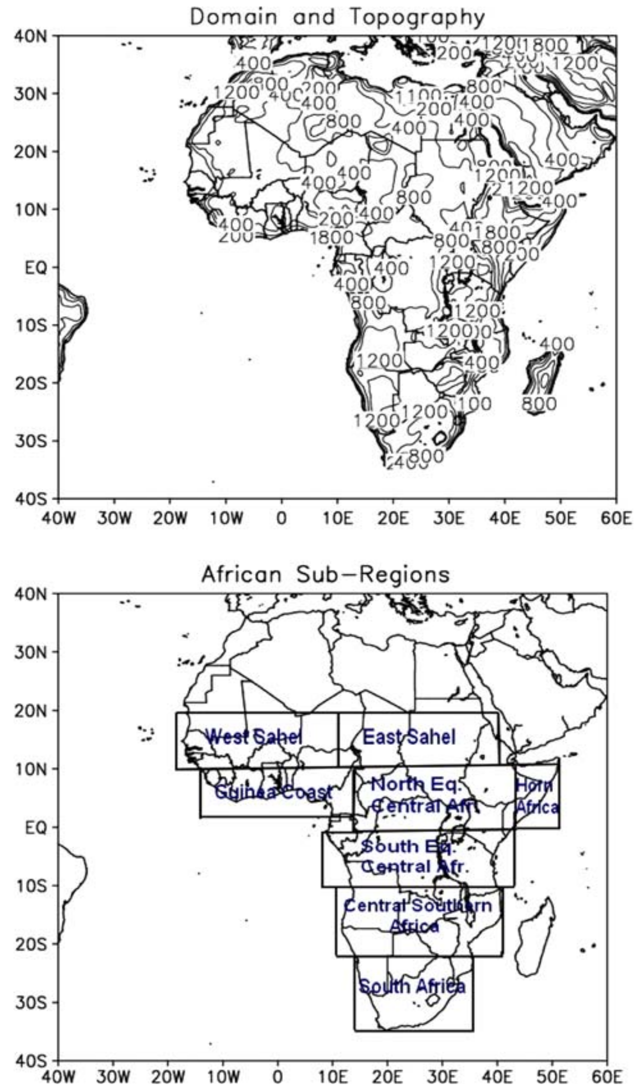

Fig. 1 Africa domain and topography (*upper panel*) and definition of the different sub-regions (*lower panel*)

4 Results

4.1 Seasonal mean climatology

4.1.1 Wind profile

The ERA-interim zonal wind profile during boreal summer (June–July–August, or JJA) averaged between 5°W and 30°E (Fig. 2a) illustrates the main dynamical large-scale features associated with precipitation over Africa north of the Equator. It exhibits a stratified structure of the atmospheric circulation locating the monsoon flow (0°–15°N) and the Harmattan fluxes (20°–30°N) at the low-level between the surface and 850 hPa, the African Easterly Jet (AEJ) at the mid-level at 600 hPa centered at 13°N and the Tropical Easterly Jet (TEJ) in the upper troposphere at 150 hPa and around 10°N.

The monsoon flow is a major source of water vapor for West Africa. The AEJ appears over Africa during the boreal summer as a result of the strong meridional surface moisture and temperature gradients between the Sahara and equatorial Africa (Cook 1999; Thorncroft and Blackburn 1999). These gradients sustain an easterly shear that is strong enough to establish the AEJ above the lower-tropospheric westerly monsoon flow. The TEJ is associated with the upper-level outflow from the Asian monsoon. RegCM3 captures the structure of these features of this atmospheric circulation. The monsoon flow and the associated westerlies are reasonably simulated both in depth and northward extent but the intensity is slightly overestimated (by 3 m/s). The AEJ is well simulated around 600 hPa but its strength is underestimated and the core is a bit shifted to the north. In the upper troposphere, RegCM3 reproduces very well the strength, location and depth of the TEJ. The shift of jet core and the overestimation of easterlies are related to an excessively strong surface temperature gradient (Cook 1999; Jenkins et al. 2005; Sylla et al. 2009; Steiner et al. 2009). Druyan et al. (2008) found that the intensity of the AEJ and TEJ simulated with their regional model (RM3) were sensitive to, and in particular increased with, vertical resolution. Here we used the standard 18 level model configurations and did not experiment with different numbers of vertical levels. Previous experience has shown that the model is not very sensitive to the number of vertical levels up to a value of 25, it is however possible that finer vertical resolution might affect the structure of the simulated jets.

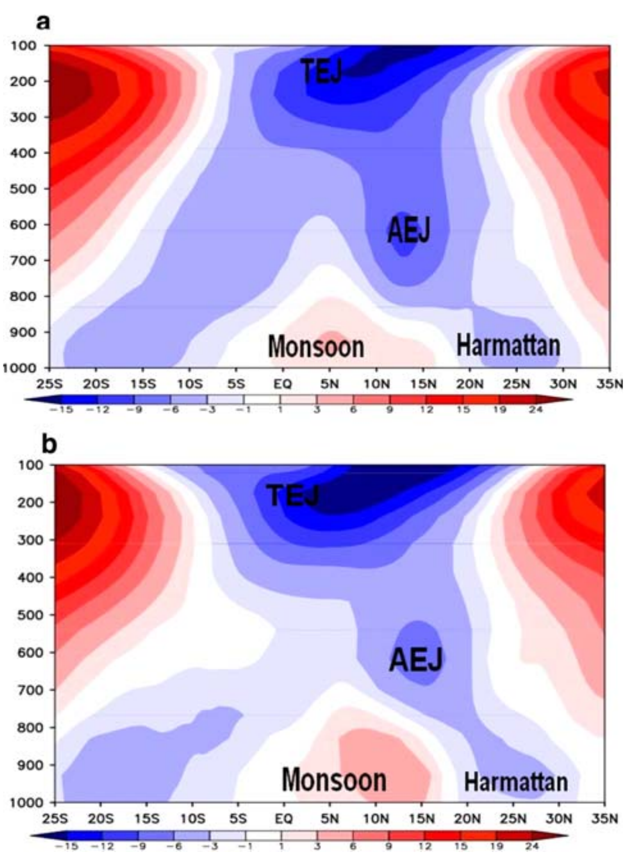

Fig. 2 Vertical cross section of the zonal wind during boreal summer (June–July–August, JJA) averaged between 5°W and 30°E for **a** ERAIM (*upper panel*) and **b** RegCM (*lower panel*). *AEJ* African Easterly Jet, *TEJ* Tropical Easterly Jet

These main circulation features are related to convective activity and rainfall over West Africa. Mohr and Thorncroft (2006) studied the relationship between the AEJ and the MCSs occurring over the region and showed that such intense systems tend to occur more frequently north of the AEJ. Most of the long-lived squall lines that cross the region are observed to occur in the vicinity of the jet (Mathon and Laurent 2001) and most of the precipitation in West Africa is associated with MCSs (D'Amato and Lebel 1998), which are organized along the AEJ (Mathon and Laurent 2001). In addition, a weak TEJ creates conditions that provide a more hostile environment for long-lived westward propagating MCSs (Squall lines, mesoscale convective complexes and non-squall tropical clusters) as they cross Africa (Janicot et al. 1996). Jenkins et al. (2005), using RegCM3, showed that the AEJ has a more equatorward position during dry years, when the TEJ is weaker than normal (Grist and Nicholson 2001). Concerning the southern Africa region, in JJA the model also reproduces the surface easterly jet south of the equator, both in location and magnitude, although the mid tropospheric easterlies are underestimated over the southern equatorial regions.

During the austral summer (DJF), the cross section of the ERA-interim mean zonal wind structure in the equatorial and southern African regions (Fig. 3a) shows easterly flow between 15° and 25°S at low levels and along the equator in the mid and upper troposphere. The low level easterlies carry water vapor from the Indian Ocean

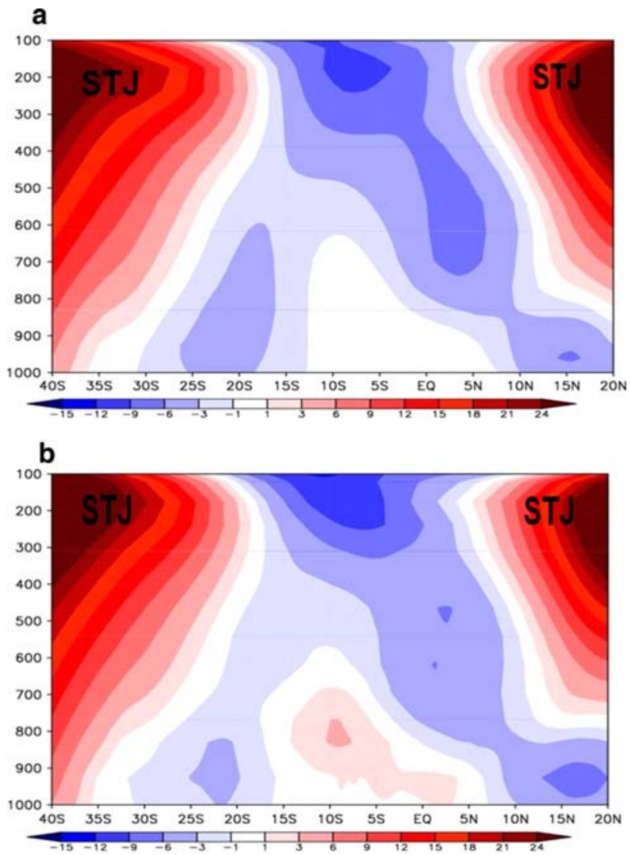

Fig. 3 Same as Fig. 2 but for Austral Summer (December–January–February, DJF). *STJ* Subtropical Jet Stream

favoring rainfall over the south equatorial African regions. At mid latitudes the upper level air flow is westerly. As shown in Fig. 3a, these westerlies are characterized by high velocities (more than 24 m/s) centered on a core jet stream that changes position throughout the year (25°S in JJA and 40°S in DJF). These strong westerlies (Subtropical Jet Stream) are maintained by the meridional temperature gradient in the mid and upper troposphere. The regional model (Fig. 3b) captures this vertical structure, locating easterlies at low levels around 20°S and at mid and upper levels along the equator. However, similarly to JJA the easterlies are weaker than observed in the equatorial mid troposphere, while the surface westerlies along the equator are somewhat overestimated compared to ERA-interim.

On the other hand, the strength, depth and extent of the South Hemisphere Subtropical Jet Stream below 100 hPa is well captured. This Subtropical Jet Stream is an important feature of the Southern Africa climate since its strength and latitude location have been linked to rainfall generation. For example, Jury et al. (1996) established the link between positive sea surface temperature (SST) anomalies over the southwestern Indian Ocean and rainfall over Southern Africa through the strengthening of the upper westerlies. They argued that the meandering of the Subtropical Jet Stream following Rossby wave activity contributes to subsidence over Southern Africa and this circulation system is anchored to an SST pattern composed of positive anomalies over the tropical Indian Ocean and negative anomalies over the tropical East Atlantic during dry years. Mwafulirwa (1999) showed that during El Niño years the stronger jet streams generated in response to the tropical warming accelerate and swerve equatorwards producing subsidence over the continental interior. Rain-bearing troughs are rapidly carried eastwards and wet spells are shorter. More recently, Reason and Rouault (2005) found that the mechanisms by which the Antarctic Oscillation influences austral winter rainfall over Southern Africa involve shifts in the Subtropical Jet Stream. In fact, wet winters were linked to equatorward shifts and stronger than average magnitude of the Subtropical Jet Stream.

Overall, the regional model is able to reproduce the dominant atmospheric circulation patterns linked to rainfall over Africa both north and south of the equator, with the main model deficiency being the underestimation of the mid-tropospheric easterlies in both seasons over the southern equatorial regions.

4.1.2 Temperature climatology

Figure 4 shows the seasonal average 2 m temperature from the CRU observations and RegCM3 simulations and the biases during the boreal (JJA) and austral (DJF) summers. In DJF (Fig. 4a), observations indicate low temperature values over northern Africa and over complex terrain regions of Guinea, Ethiopia, Cameroun, Tanzania, Angola and South Africa highlands. The highest values are along the Guinea Coast, the areas south of Sudan and the southern Horn of Africa. RegCM3 (Fig. 4c) reproduces well this spatial pattern but it extends slightly to the south the area of minimum temperature over northern Africa. In MAM (not shown), CRU gives more or less the same spatial distribution but shows a band of warm temperatures in the Sahel (10°–20°N) extending from West to East Africa which RegCM3 captures. In JJA and SON (not shown), CRU (Fig. 4b) and RegCM3 (Fig. 4d) are in good agreement. They both locate peaks of high temperatures in the Sahara desert (northern Sahel and southern Sahara). For both seasons, the lowest temperatures are found over orographic regions of South Africa. However, in JJA the regional model tends to underestimate temperatures around the complex terrains of West Africa (Guinea Highlands and Cameroun mountains) and to overestimate them in the Congo Basin and south of Sudan.

Overall, in DJF the temperature biases are low, mostly between −2 and 2°C. Positive biases are mainly located over the tropical forest regions while negative biases are found in northern Africa in the Sahara desert. In JJA, the

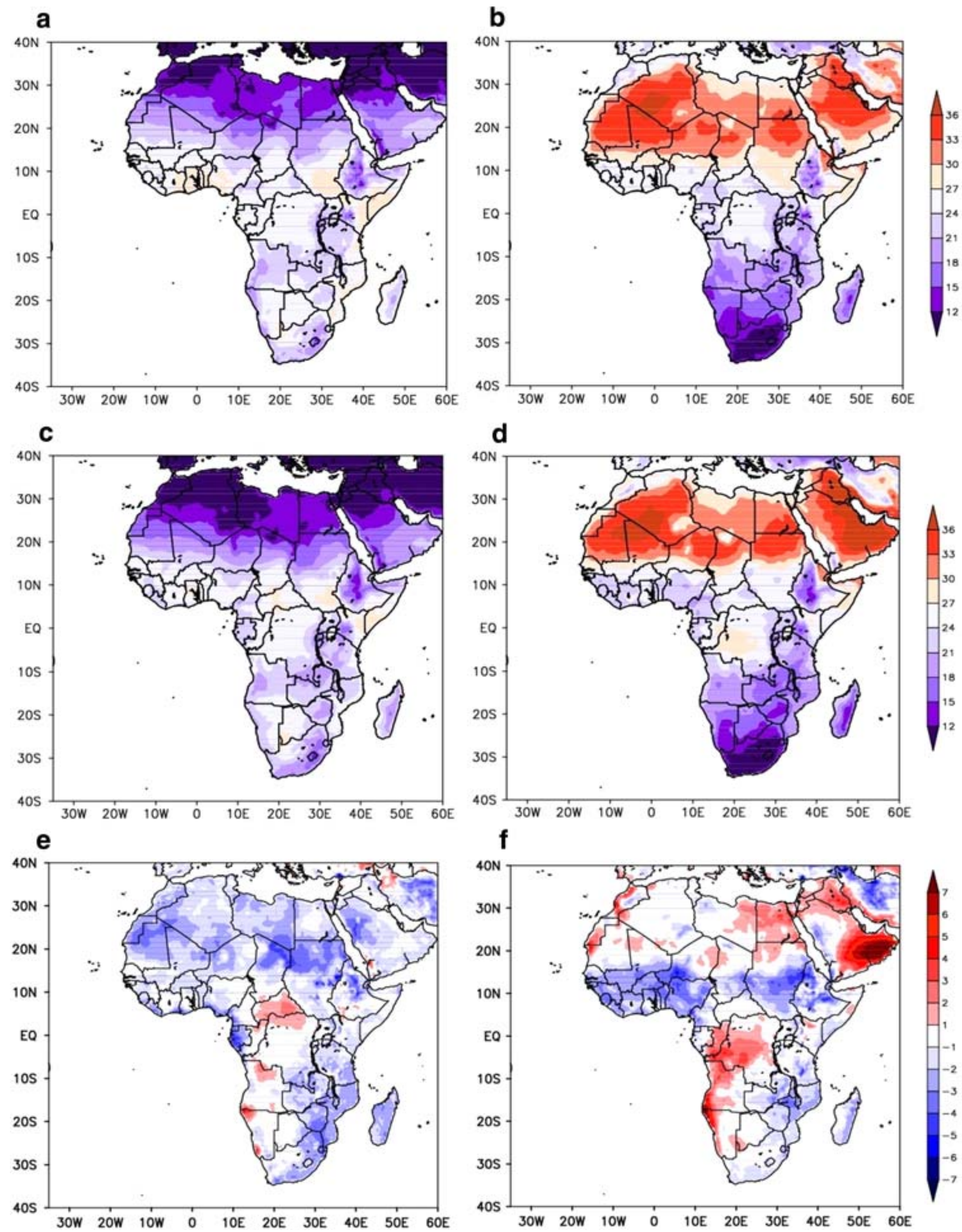

Fig. 4 Averaged 1989–2002 two-meter air temperature (in °C) in DJF (*left panels*) and JJA (*right panels*) from CRU (*upper* **a** and **b**) and RegCM (middle **c** and **d**), along with the RegCM minus CRU difference (*lower panels* **e** and **f**)

model overestimates temperatures in the Congo Basin, Angola highlands and Namibia desert and underestimates them north of the equator in the convective regions along the ITCZ. Only few small regions exceed 2°C of bias. In particular, the biases over the Guinea region and southern Sahel have been shown not to depend on the boundary forcing (Sylla et al. 2009). Note that the underestimation of temperature over the complex terrain of Guinea in JJA may lead to an increased north-south temperature gradient between Guinea and the Sahara, which may be responsible for the stronger monsoon flow and the slight shift of the AEJ core found in the regional model.

It is difficult to unambiguously determine the causes of the model temperature biases, since these may depend on a number of factors, including cloudiness, temperature advection and surface water and energy fluxes. In a number of short sensitivity tests we found that the simulated temperature is sensitive to quantities such as surface albedo, vegetation type, and stomatal resistance, but the effect of these quantities varies from region to region. In addition, dust and aerosols affect the surface incoming radiation (Konare et al. 2008) and, as a consequence, also surface temperature. Considering these uncertainties, and considering that typical RCM biases for seasonal surface temperature are within the range of 2°C (e.g. Jones et al. 1995; Giorgi et al. 1998; McGregor et al. 1998; Hudson and Jones 2002), our model biases are in line with those of other state-of-the-art regional models.

4.1.3 Precipitation climatology

In this section we examine the spatial patterns of seasonal precipitation and the associated low level circulation. Figure 5 compares DJF and JJA averaged CRU precipitation (Fig. 5a, b), GPCP precipitation and the ERA-interim winds at 925 hPa (Fig. 5c, d) with the corresponding RegCM3 fields (Fig. 5e, f). In DJF, the ICTZ approaches its southernmost location. Therefore, observed precipitation (CRU and GPCP) (Fig. 5a, c) over the continent is mostly confined to South Equatorial Central Africa and Central Southern Africa, while regions north of the equator are predominantly dry. This precipitation pattern is associated with moist southeasterly winds over the southern Indian Ocean and northeasterlies over the northern Indian Ocean converging over South Equatorial Africa and generating intense convection there. In the northern hemisphere, winds are mainly dry northeasterlies. In addition, the eastern periphery of the anti-cyclonic flow in the South Atlantic subtropical high converges with the easterlies from the north Atlantic Azores high to generate an area of heavy rainfall in the equatorial Atlantic ocean. In MAM (not shown), the ICTZ moves equatorwards and precipitation is confined to the Gulf of Guinea and South Equatorial Central Africa. Wind patterns are mainly the same as in DJF except that the north-easterlies over the northern Indian Ocean cease and strong southeasterly winds drift in.

The regional model reproduces the major features of precipitation and low level circulation in both seasons (DJF and MAM). However, the model is drier than observed in the convergence zone of the equatorial Atlantic and wetter in the Indian Ocean north of Madagascar. The dry bias is connected to weaker easterlies from the north and south

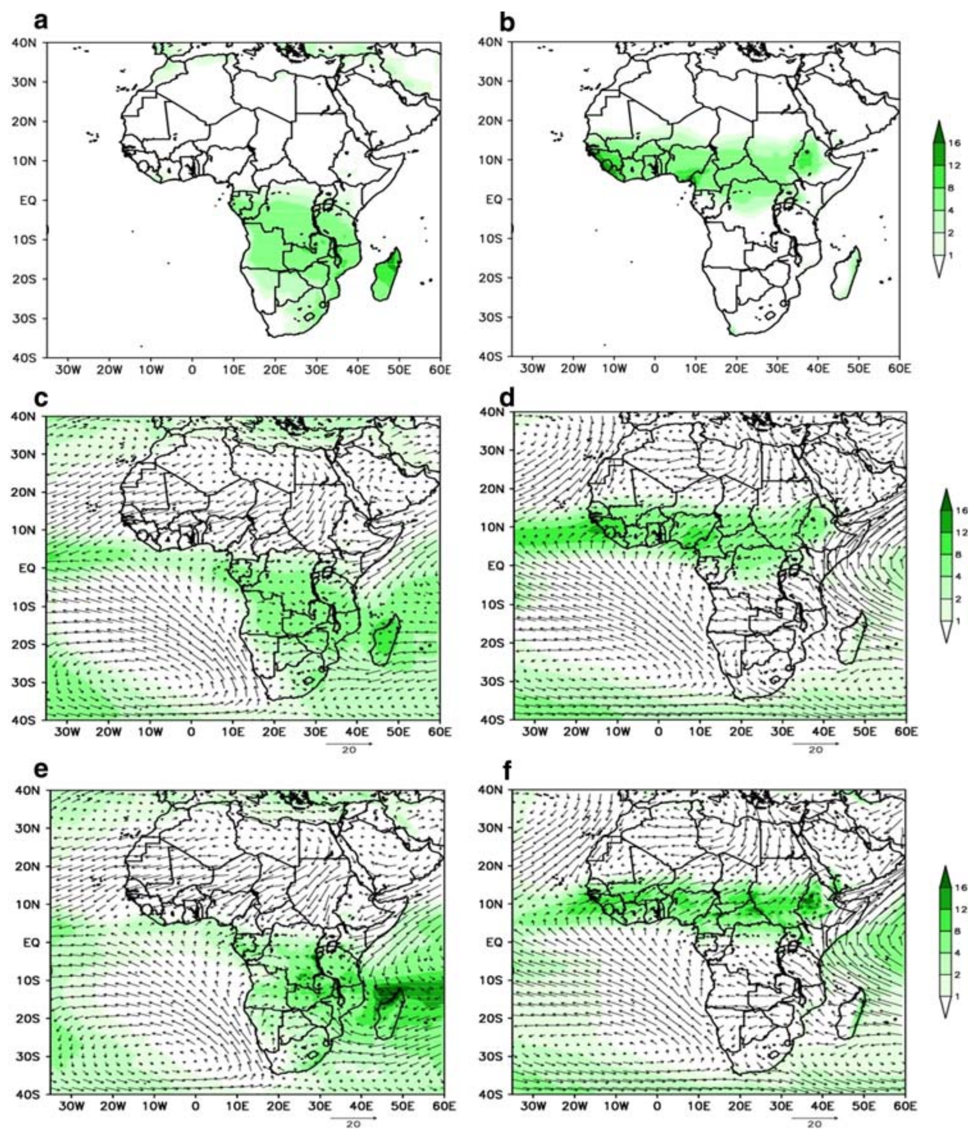

Fig. 5 Averaged 1989–2005 precipitation (in mm/day and shaded) from CRU (*upper panels* **a** and **b**), GPCP with superimposed ERAIM 925 hPa wind vectors (*middle panels* **c** and **d**) and RegCM3 with superimposed 925 hPa wind vectors (*lower panels* **e** and **f**) in DJF (*left panels*) and JJA (*right panels*)

Atlantic while the wet bias seems to be associated to stronger easterlies in the Indian Ocean. Over the African continent the main precipitation bands are well captured by the model.

In JJA, the ITCZ is at its northernmost position and the West African monsoon rainfall is at its maximum. CRU and GPCP locate precipitation in a zonal band between the equator and 15°N, in which rainfall decreases northwards. This precipitation is mainly associated to the frequent occurrence of propagating MCSs related to the above described dynamics of the AEJ and TEJ (Jenkins et al. 2005; D'Amato and Lebel 1998). In addition, CRU depicts three peaks of rainfall around the Guinea Highlands, Cameroun Mountains and Ethiopia Highlands which are connected to orographic features. Due to its coarse resolution, GPCP does not show any heavy rainfall over the Ethiopia Highlands. The associated low level circulation in ERA-interim shows north and south Atlantic anti-cyclonic flows, the West African monsoon flow as well as northerlies and easterlies around the Saharan thermal low region. In SON (not shown), the ITCZ retreats southward and the monsoon flow becomes weaker.

RegCM3 reproduces quite well the low level circulation features for both seasons (JJA and SON) with a slight overestimation of wind intensity in the northern Sahel in JJA. Precipitation patterns are well captured. The width of the rain belt and location of maxima are well represented in the simulation, but the intensity is slightly overestimated over southern Sudan in JJA and over the central African tropical forest in SON (not shown). In addition, RegCM3 shows small scale peaks of rainfall not appearing in GPCP over some orographic zones such as the Jos Plateau, northern Chad and the East African highlands. The precipitation maximum over Ethiopia is clearly depicted in CRU. The discrepancies evident between the GPCP and CRU datasets confirms that significant uncertainties are present in observed precipitation climatologies (Vizy and Cook 2002). Therefore, the RegCM3 simulation of rainfall appears to be within this range of uncertainty.

Previous studies have shown that the simulation of African precipitation by RegCM3 is sensitive to the physics parameterizations used. Pal et al. (2007) used RegCM3 driven by ERA-40 in a similar domain and with the same resolution (50 km), but using the convection scheme of Emanuel and Rothman (1999). They found that the model simulated excessive precipitation over the wettest areas, and the core of the monsoon rain belt was simulated a few degrees too far north over West Africa in JJA. Furthermore, the intensity of the winds that enter the Guinea coast was too high. Steiner et al. (2009) replaced BATS in the model configuration of Pal et al. (2007) with the Common Land Surface scheme and found that the simulation of precipitation considerably improved through a better description of the surface energy and water budgets and related gradients. Vizy and Cook (2002) used a modified version of the MM5 driven by ERA-40 in a relatively smaller domain and found the opposite: the northward component of the low-level flow was weaker than observed and associated monsoon rain belt was located too far south.

Additional RCM studies have been carried out with RegCM3 using a smaller domain centered over eastern Africa and most of them found difficulties to correctly reproduce the precipitation patterns. For example, Segele et al. (2008) performed 18 years of simulation with RegCM3 over eastern Africa and overestimated by 50% (26%) precipitation over Ethiopia when using the Grell (Emanuel) convective scheme. Anyah and Semazzi (2007) completed a multiyear simulation of the short east Africa rainy season using RegCM3 and found deficiencies in capturing the observed rainfall over the Kenya Highlands and Lake Victoria Basin. Sun et al. (1999a) simulated the short rainy season of 1988. Not only some deficiencies over the Congo-Angola Basin and Kenya Highlands were shown, but also the monsoon flow during that period was stronger than observed. Other regional model studies experienced difficulties in simulating precipitation over Africa. Paeth et al. (2005) underestimated total precipitation by up to 25% over southern West Africa using REMO. Gallée et al. (2004), using MAR, overestimated precipitation in August and the precipitation maxima along the coast near Guinea/ Sierra Leone and Cameroon were not captured well. Jung and Kunstmann (2007) used MM5 over the Volta region and found an underestimation of coastal rainfall.

All these experiments show that it is extremely difficult to simulate well African precipitation. Part of the relatively good performance of our simulation can certainly be ascribed to the use of ERA-interim reanalysis to drive our model at the lateral boundaries. However, although difficult to unambiguously assess without targeted sensitivity experiments, the choice of physics parameters, convection scheme (see Sect. 2) and possibly large domain also contribute substantially to the model systematic errors.

Although it is difficult to determine unambiguously the origins of temperature and precipitation biases, cloudiness is a key factor and may play an important role in the distribution of these quantities. Figure 6 compares the distribution of the fraction of cloud cover (in percent) from CRU observations (Fig. 6a, b) and RegCM3 simulations (Fig. 6c, d) for DJF and JJA respectively. During DJF, as expected, CRU observations locate the maximum cloud cover in the Southern Hemisphere, especially over the South Equatorial Central Africa and Central Southern Africa and the minimum cloud cover north of the Equator, consistently to precipitation distribution. RegCM3 reproduces quite well the spatial distribution but slightly overestimates cloud cover over northern Africa and

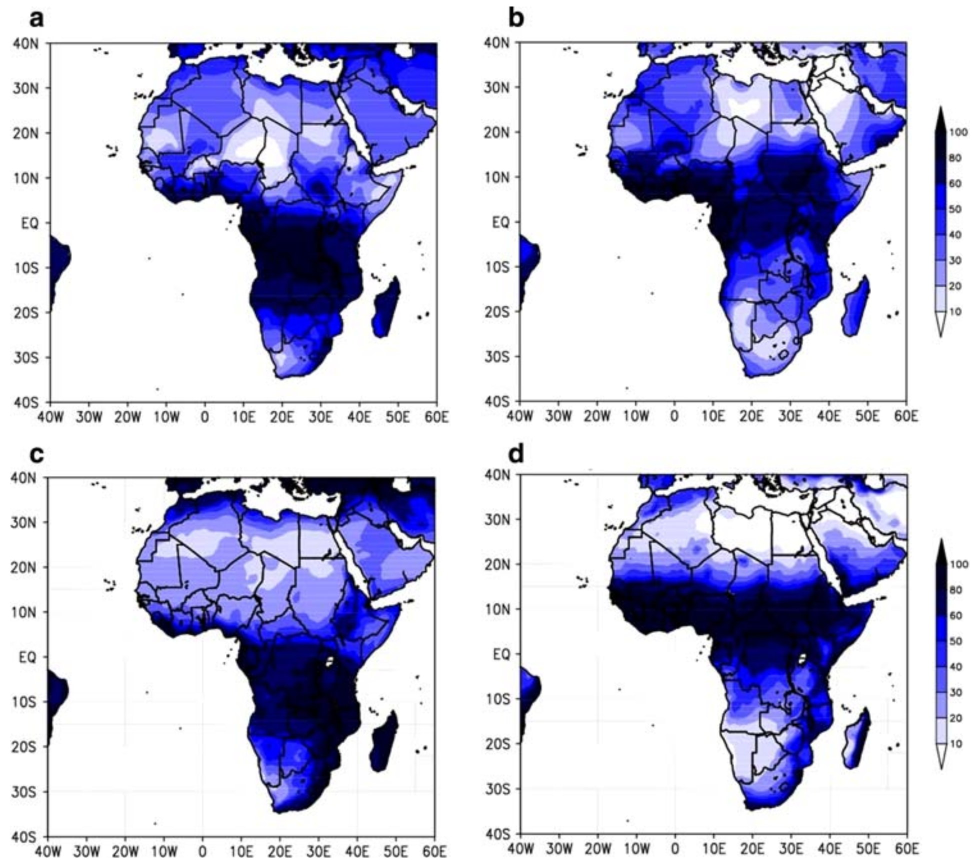

Fig. 6 Averaged 1989–2002 cloud cover fraction (in percent) from CRU (*upper panels* **a** and **b**), and RegCM3 (*lower panels* **c** and **d**) in DJF (*left panels*) and JJA (*right panels*)

underestimates in the Sahara, the Sahel and around northern Angola. This latter underestimation is connected to some dry biases in precipitation and warm biases in temperature. During JJA, CRU observations show the maximum of cloud cover in a zonal band along the equatorial regions. North and South of these regions, cloud cover decreases zonally. This spatial pattern is also similar to the precipitation one. The regional model finds the zonal variation of the cloud cover distribution but underestimates it over the Sahara and overestimates it in the convective region (along the ITCZ) and especially in the orographic zones inside. This overestimation is associated to the cold biases in temperature simulated by RegCM3 in these regions. This does not cause systematiquely an overestimation of rainfall (see for example the Niger basin in western Africa). However, RegCM3 shows some maxima of rainfall, not appearing in the CRU observation, or overestimates them in regions of complex terrains inside the ITCZ (Ethiopian Highlands) where the problem may be artificially enhanced by the lack of a gauge under-catch correction in the observed data.

Globally, the overestimation (underestimation) of cloud cover seems to be related to an underestimation (overestimation) of surface temperature and overestimation (underestimation) of precipitation especially in the orographic regions compared to observations. This is in line with Pal et al. (2000) and Coppola and Giorgi (2009).

4.2 Precipitation temporal variability

4.2.1 Mean annual cycle

In this section we analyze the mean annual cycles of RegCM3-simulated precipitation for the eight subregions defined in Fig. 1b and compare them to different sets of observations (GPCP, CRU and FEWS) and to the ERA-interim reanalysis. The annual cycle values are averaged for each sub-region of Fig. 1 (land only) over the whole simulation and observation periods (See Table 1). According to GPCP, CRU and FEWS, the West Sahel (WSA) annual cycle (Fig. 7a) peaks in August with some slight differences in the intensities among the observed estimates. RegCM3 and ERA-interim both reproduce the

Table 1 Summary of available observational data and their temporal coverage

Data	RegCM3	ERAIM	GPCP	CRU	FEWS
Period	1989–2005	1989–2005	1989–2005	1989–2002	2001–2005

observed peak in August but RegCM3 tends to overpredict its magnitude while ERA-interim tends to underpredict it. The same behavior is found over the East Sahel (ESA) region (Fig. 7b), except that the observed intensities are lower than over the West Sahel and RegCM3 (and to a lesser extent ERA-interim) still overestimates the precipitation peak.

Over the Guinea Coast (GCO; Fig. 7c) all the observational datasets show a primary maximum in April–June, a secondary one in September–October and a relative minimum in mid-summer, as the monsoon rainband seasonally migrates in the north–south direction. However, there is a wide spread in the magnitude and phase of the precipitation maxima across these datasets, with the CRU showing the largest magnitudes, FEWS the smallest and GPCP some intermediate values. The ERA-interim captures the two maxima, but tends to overestimate precipitation compared to all observation datasets, except for the CRU in July through September. RegCM3 also captures well the two maxima, it produces lower precipitation

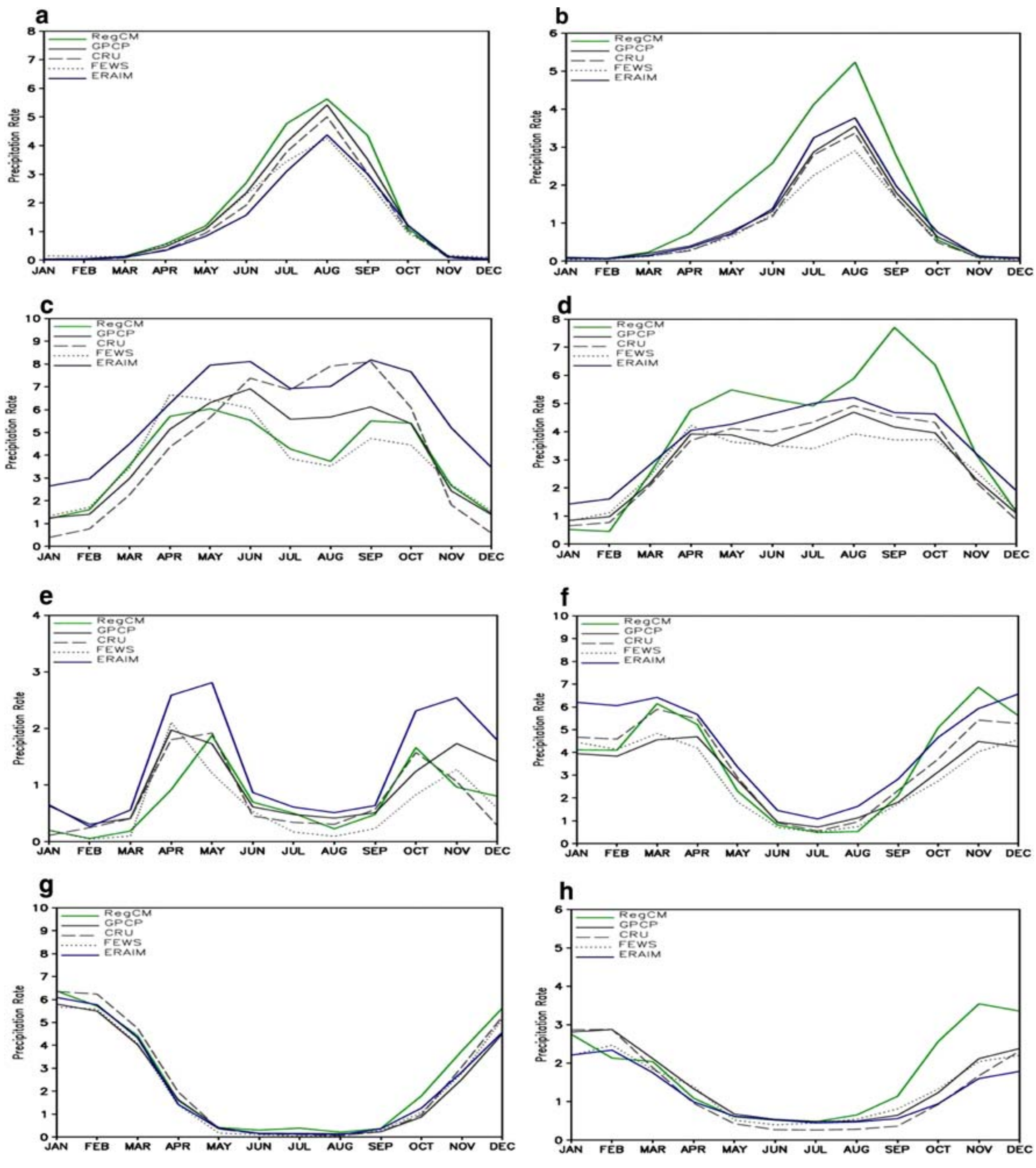

Fig. 7 Averaged precipitation annual cycle (in mm/day) from RegCM (*green*), GPCP (*black solid*), CRU (*dashed*), FEWS (*dotted*) and ERAIM (*blue*) over **a** West Sahel; **b** East Sahel; **c** Guinea Coast; **d** North Equatorial Central Africa; **e** Horn of Africa; **f** South Equatorial Central Africa; **g** Central Southern Africa; **h** South Africa

amounts than ERA-interim and it is in close agreement with the FEWS data, both in terms of magnitude and phase of the maxima and minima. Two precipitation maxima are also found in North Equatorial Central Africa (NEC; Fig. 7d), but the observed peaks as well as the minimum are much less pronounced. RegCM3 captures this double-peaked structure, but overestimates its magnitude, especially in the fall. Conversely, ERA-interim has precipitation values closer to observed, but does not capture the double peaked seasonal structure.

The double-rainy season structure is marked over the Horn of Africa (HOA; Fig. 7e), with the two rainy seasons occurring in April–May and October–December and being separated by a very dry season in June–September. This double-peaked structure is associated with a north–south migration of the ICTZ that sweeps this and adjacent equatorial regions (Adefolalu 1974; Adegoke and Lamptey 2000). All the observed and model datasets capture this structure, however with some variability in the phase and magnitude of the maxima. In particular, the ERA-interim overestimates the magnitude of the precipitation maxima and RegCM3 tends to agree best with the CRU data. A generally good agreement between all observed and modeled datasets is instead found over the South Equatorial Central Africa (SEC; Fig. 7f), where the precipitation seasonal cycle is characterized by two peaks in March and November separated by very dry summer months. In this case the ERA-interim fails to capture the relatively dry conditions in December through January. Finally, both southern regions (Central South Africa: CSA; South Africa: SOA) show a pronounced seasonal cycle with a maximum in November through March and a minimum in May through September. RegCM3 and ERA-interim capture this structure well in both regions (especially over Central South-Africa, Fig. 7 g), although the regional model overestimates the Austral summer maximum over the South Africa region.

Overall, RegCM3 performs well in reproducing the seasonal cycle of precipitation over all regions, except for an overestimation of the magnitude of the peak over the East Sahel, North Equatorial Central-Africa and Southern Africa regions. We note that, although they refer to different periods (See Table 1), the observation datasets do not always agree in the magnitude and especially the phase of the rainy season peaks and corresponding breaks, which adds an element of uncertainty in the evaluation of the model. We also find that in a number of instances RegCM3 is actually capable of producing phases and/or magnitudes of peaks more in agreement with the observational datasets than the ERA-interim.

Comparison with previous studies shows varying degrees of improvement in the timing and magnitude of the annual cycle over some sub-regions. For example, over the Guinea Coast Afiesimama et al. (2006) (using the NCEP reanalysis at the lateral boundaries) shifted the first peak to July and overestimated precipitation by about 5 mm/day during the rainy season. Sylla et al. (2009), when forcing RegCM3 with NCEP reanalysis and ECHAM5 global model, respectively, displaced the Guinea Coast minimum to August and September compared to the CRU observations. Pal et al. (2007) overestimated significantly the peaks of rainfall over the Guinea Coast and the Sahel when using RegCM3 with the Emanuel convection scheme. In general, we thus find that the present simulation is of relatively good quality with respect to previous RegCM simulations.

Finally, from this analysis, a set of rainy seasons can be defined for each subregion. WSA, ESA, CSA and SOA are far away from the equator and have only one rainy season, while the equatorial regions (GCO, SEC, NEC and HOA) experience two rainy seasons due to the north–south migration of the ITCZ. The rainy seasons over different sub-regions are summarized in Table 2 and used for the analysis shown in the next section.

Table 2 Summary of the different rainy season for each sub-region of Fig. 1

Sub-regions	WSA	ESA	GCO	NEC	SEC	HOA	CSA	SOA
First rainy season	JAS	JAS	MJJ	AMJ	FMA	MAM	DJF	DJF
Second rainy season			ASO	ASO	NDJ	SON		

JAS July–August–September, *MJJ* May–June–July, *AMJ* April–May–June, *FMA* February–March–April, *MAM* March–April–May, *DJF* December–January–February, *ASO* August–September–October, *NDJ* November–December–January, *SON* September–October–November

4.2.2 Interannual variability

Figures 8 and 9 show simulated and observed rainfall anomalies over the eight climate sub-regions of Fig. 1 and for the rainy seasons identified in (Table 2). As reference in the figure we use the GPCP data, which is the only observational dataset that includes the full simulation period. The anomalies are calculated with respect to the precipitation mean derived from the full 17 year period 1989–2005. The area averages of precipitation anomalies are normalized by the standard deviation derived from the 1989–2005 time series. Table 3 summarizes the correlation coefficients between simulated and observed anomalies as well as the difference between simulated and observed interannual coefficient of variation (interannual standard deviation divided by the mean), which we here take as a measure of interannual variability.

Figure 8 first shows the interannual anomalies for the ERA-interim (a, c, e and g) and RegCM3 (b, d, f and h)

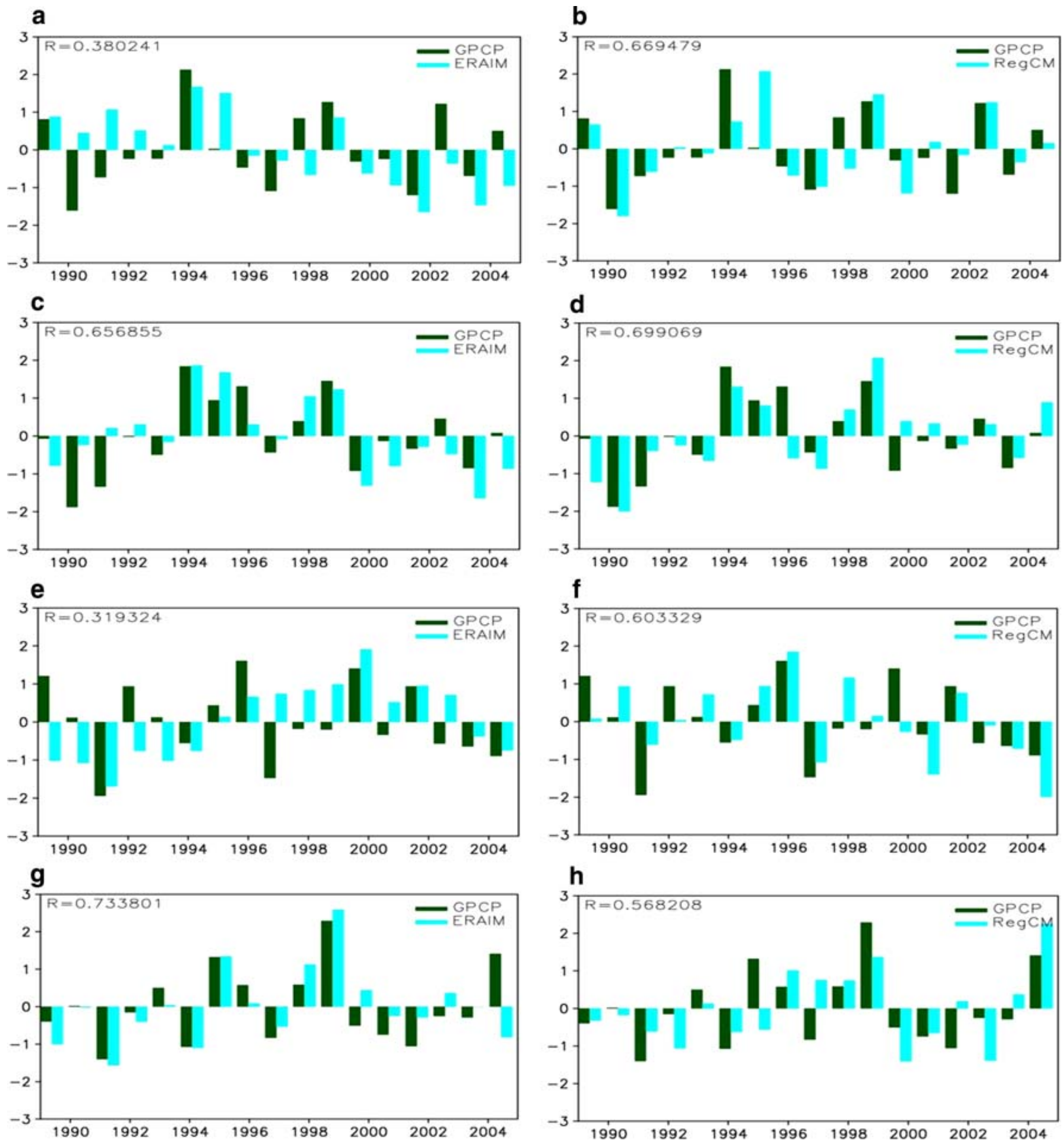

Fig. 8 Normalized precipitation anomaly for the rainy season of sub-regions away from the equator: WSA (**a**, **b**); ESA (**c**, **d**); CSA (**e**, **f**); SOA (**g**, **h**) for GPCP versus ERAIM (*left panels*) and GPCP versus RegCM (*right panels*)

precipitation compared to GPCP in the subregions far away from the Equator. ERA-interim fails to reproduce the interannual variability over the West Sahel and Central South Africa but captures it fairly well over the East Sahel and South Africa, with correlation coefficients approaching 0.65 and 0.73, respectively. We also note that the failure (success) of ERA-interim to consistently reproduce the interannual variability is connected to a strong (weak) overestimation/underestimation of the coefficient of variation compared to the observations (see Table 3). Over these regions the RegCM3 simulation generally captures well both the occurrence of individual anomalies (correlation coefficients of 0.56–0.7) and the coefficient of variations (errors in the range of 11–43% errors). Simulated interannual variability in all these semi-arid subregions thus agrees with observations. Also note that over the West Sahel and Central South Africa, RegCM3 actually improves the results from ERA-interim, both for the correlation coefficient and the coefficient of variation.

Over the equatorial subregions (GCO, NEC, SEC, HOA), only one of the two rainy seasons is presented (ASO for GCO, ASO for NEC, FMA for SEC and SON for HOA) but the correlation coefficients of all rainy seasons and their coefficients of variation are summarized in Table 3. As

Fig. 9 Normalized precipitation anomalies during one rainy season for sub-regions close to the equator: GCO (**a**, **b**); NEC (**c**, **d**); SEC (**e**, **f**); HOA (**g**, **h**) for GPCP versus ERAIM (*left panels*) and GPCP versus RegCM (*right panels*)

Table 3 Correlation coefficients and differences between the coefficients of variation (ERAIM or RegCM minus GPCP) in each sub-region of Fig. 1 and rainy season

Sub-region		WSA	ESA	GCO		NEC		SEC		HOA		CSA	SOA
Correlation coefficient with respect to GPCP	ERAIM	0.38	0.66	0.77	0.57	−0.09	0.38	0.46	0.60	0.57	0.92	0.32	0.73
	RegCM	0.67	0.70	0.55	0.45	0.24	0.44	0.38	0.32	−0.35	0.81	0.60	0.57
Difference coefficient variation in % with respect to GPCP	ERAIM	72	−3	−28	−23	−18	15	−54	−26	32	−13	44	27
	RegCM	−36	43	51	−50	−40	26	−22	−3	24	−48	−11	−16

shown in Fig. 9, over these regions and rainy seasons, results are more varied, with correlation coefficients in the range of 0.38–0.91 and a general consistency between the ERA-interim and RegCM3 values. Note, in particular, the very high correlations over the Horn of Africa region, 0.92 in ERA-interim and 0.8 in RegCM3. Consistently with these results, the error for the coefficient of variation is relatively low (mostly less than 30%). For the rainy seasons not shown in Fig. 9 (see Table 3), we find correlation coefficients in the range of 0.3–0.6 except for the three noticeable cases of NEC in ERA-interim and RegCM3 and HOA in RegCM3, where essentially the sequence of observed anomalies is not captured.

Overall, Figs. 8 and 9 and Table 3 indicate that, except for a few cases, both the ERA-interim and RegCM3 are able to capture the observed anomalies as well as the magnitude of interannual variability (measured by the coefficient of variation). Also, the results are mostly in line between the ERA-interim and RegCM3, a result of the lateral forcing by the reanalysis fields. However, a few exceptions occur, especially over some equatorial regions where the correlations are relatively low. For a large domain such as the one used here, the boundary forcing may not be strong near the central equatorial regions and local model-simulated processes may become dominant. Indeed over these regions (HOA and NEC in their first rainy season), although the correlations are low the error on the coefficient of variation is in line with that of the other regions, indicating that the model does not capture specific individual events but captures the observed magnitude of interannual variability. This would be sufficient for application to climate studies.

Direct comparison with previous regional model interannual variability studies over Africa is difficult, as the sizes of the subregions and the seasons considered differ from study to study. Nonetheless, Sun et al. (1999b) completed 12 years of simulations and found a significant correlation (0.8) over Tanzania while validating their model simulation against gridded and local station data. In addition, when dividing the Kenya Highlands into two regions (East and West), the western highlands showed a good correlation (0.847), while the regional model failed to capture the interannual variability over the eastern highlands (correlation of 0.45). Afiesimama et al. (2006) found correlation coefficients of 0.51, 0.62 and 0.65 between RegCM3 simulated and observed anomalies over the Guinea Coast, West and Central Soudano-Sahel subregions, respectively, for June–September. Anyah and Semazzi (2007) correlated rain-gauge data with their RegCM3 simulations over East Africa and found that only one station (Central Tanzania) was able to reach a correlation of 0.7 during the short rainy season of October–December while a station over Central Kenya showed a poor correlation (0.2). More recently, Steiner et al. (2009) compared their simulated interannual variability with both CRU and CMAP precipitation anomalies and obtained correlations of up to 0.5 over the Guinea Coast and the Sahel. Our results are thus in line and often better than previous ones using smaller domains and older reanalysis boundary conditions.

5 Summary and conclusions

In this paper we evaluated the performance of RegCM3 in reproduce observed climatology, seasonal cycle and interannual variability of temperature and precipitation over a large domain covering the entire African continent, with the model being driven by the recently produced ERA-interim reanalysis. We analyse results spatially over the whole domain and averaged over eight climate sub-regions identified in Fig. 1. Note that the large domain used in this work allows more freedom for the regional model to produce its own circulations, especially in the middle of the domain, and therefore this validation analysis provides a stringent test of the model performance.

Our results show that the regional model is able to capture fairly well the main circulations influencing the African continent, such as the monsoon flow in the lower troposphere, the AEJ and TEJ in the mid and upper troposphere for the boreal summer north of the equator. In the austral summer, the Subtropical Jet Stream, the low level easterlies and the mid and upper troposphere easterlies are also captured. The main systematic errors in the RegCM3 simulation are an overestimate of the strength of the monsoon flow and an underestimate and slight northward displacement of the AEJ core compared to the driving ERA-interim reanalysis. The stronger monsoon flow and the shift of the AEJ are related to an overestimation of the low level temperature gradients when compared to ERA-interim. The model also somewhat underestimates the intensity of easterlies in the mid-troposphere.

Simulated seasonal rainfall climatologies are generally consistent with observations. RegCM3 captures the spatial variability of rainfall, the north–south migration of the ITCZ and the associated low level circulation. Maxima are well represented over complex terrains, although the model tends to overestimate precipitation over tropical high elevation mountain areas. This has been found also in other applications (e.g. the tropical Andes) although over these regions observed estimates may be affected by a high uncertainty due to the paucity of high elevation stations. The regional model tends to overestimate precipitation over south Sudan and the equatorial tropical forest in JJA and SON, respectively. This is consistent with a model underestimation of 2 m temperature which may be due to an overestimation of cloud cover or an excessive surface evapotranspiration. Nevertheless, our regional model performance appears improved compared to that of Pal et al. (2007) and previous RegCM3 studies over Africa carried out using smaller domains and older reanalyses for the provision of lateral boundary conditions.

The mean annual cycles over different climate subregions show that the equatorial regions (GCO, NEC, SEC and HOA) are characterized by two rainy seasons associated with the north–south migration of the ITCZ, while the regions far away from the equator (WSA, ESA, CSA and SOA) have only one rainy season related to the onset and evolution of regional monsoon circulations. RegCM3 reproduces well the amplitude and phase of rainy and dry seasons for all the subregions except for a few cases when the magnitude of the peaks is overestimated. In particular, the regional model is shown to perform even better than the reanalysis in a number of the subregions.

Finally, the RegCM3 simulation captures relatively well the interannual variability of the rainy seasons over most subregions analyzed, both in terms of statistical values and individual anomalies. Exceptions are two equatorial regions near the center of the domain, where the correlations with observed anomalies are low, but the error of statistical variability is also low. In these cases, evidently local model processes are more important than the lateral boundary forcing in determining the precipitation variability.

Overall, the simulation analysed here indicates a relatively good performance of the RegCM3 over a large African domain encompassing the entire continent and adjacent ocean water. Part of this relatively good performance (compared to previous model experiments) is due to the use of ERA-interim to produce improved lateral boundary conditions. Choice of domain, convection scheme and some parameter values also contributed to this improvement, although it is difficult to clearly identify the contributions of these different elements. It is interesting to note that our dynamical downscaling is able to improve some aspects of African rainfall with respect to ERA-interim, most noticeably over West Africa, which lies away from the eastern boundary where most of the westward moving variability (Rossby Waves) is generated and influences the African Easterly Waves genesis (Thorncroft and Kiladis 2008). An important point regarding model validation is that we employed three different observational datasets. In some areas they do show a good level of agreement, but in others they show a relatively wide spread. This indicates a substantial uncertainty in observed estimates of precipitation which should be taken into account when evaluating climate models over the African continent.

Because of our large domain, we used a grid spacing of 50 km, but we do plan to extend our analysis to a higher resolution model configuration. Also, we plan to use this model configuration to produce new sets of high resolution climate change scenarios over Africa and to study aerosol and land surface effects over the African continent under the regional climate change hyper-matrix framework (Giorgi et al. 2008) and the coordinated regional climate downscaling experiment (CORDEX, Giorgi et al. 2009).

Acknowledgments Support was provided by ENEA, ICTP and AMMA-EU program (African Monsoon Multidisciplinary Analysis). The computations for this project were performed at ENEA, Casaccia Center (Roma-Italia). Therefore, authors would like to acknowledge gratefully the assistance and technical support provided by the system manager Emmanuele Lombardi (Lele). Thanks also to the two reviewers whose comments significantly improve the quality of the manuscript.

References

Abiodun BJ, Pal JS, Afiesimama EA, Gutowski WJ, Adedoyin A (2007) Simulation of West African monsoon using RegCM3 Part II: impacts of deforestation and desertification. Theor Appl Climatol 93:245–261

Adefolalu DO (1974) On scale interactions and the lower tropospheric summer easterly perturbations in tropical West Africa. Ph.D. thesis, FSU, Tallah, Fla, p 276

Adegoke JO, Lamptey BL (2000) Intraseasonal variability of summertime precipitation in the Guinea coastal region of West Africa. In: Proceedings of the workshop on the West African monsoon variability and predictability. WMO-TD No. 1003, pp 115–118

Adler RF et al (2003) The version-2 Global Precipitation Climatology Project (GPCP) monthly precipitation analysis (1979-present). J Hydrom 4(6):1147–1167

Afiesimama AE, Pal JS, Abiodun BJ, Gutowski WJ, Adedoyin A (2006) Simulation of West African monsoon using the RegCM3. Part I: model validation and interannual variability. Theor Appl Climatol 86:23–37

Anyah RO, Semazzi FHM (2007) Variability of East African rainfall based on multiyear RegCM3 simulations. Inter J Climatol 27:357–371

Cook KH (1999) Generation of the African Easterly Jet and its role in determining West African precipitation. J Clim 12:1165–1184

Coppola E, Giorgi F (2009) An assessment of temperature and precipitation change projections over Italy from recent global and regional climate model simulations. Inter J Climatol. doi: 10.1002/joc.1867

D'Amato N, Lebel T (1998) On the characteristics of the rainfall events in the Sahel with a view to the analysis of climatic variability. Inter J Climatol 18:955–974

Dickinson RE, Henderson-Sellers A, Kennedy PJ (1993) Biosphere–atmosphere transfer scheme (BATS) version 1E as coupled to the NCAR Community Climate Model. Technical Note NCAR/TN-387+STR, p 72

Diffenbaugh N, Pal J, Trapp R, Giorgi F (2005) Fine-scale processes regulate the response of extreme events to global climate change. Proc Natl Acad Sci USA 102(44):15774–15778

Diongue A, Lafore JP, Redelsperger JL, Rocca R (2002) Numerical study of a Sahelian synoptic weather system: initiation and mature stages of convection and its interactions with the large-scale dynamics. Q J R Meteorol Soc 128:1899–2007

Druyan LM, Fulakeza M, Lonergan P (2008) The impact of vertical resolution on regional model simulation of the West African summer monsoon. Int J Climatol 28:1293–1314

Emanuel KA, Rothman MZ (1999) Development and evaluation of a convection scheme for use in climate models. J Atmos Sci 56:1756–1782

Fritsch JM, Chappell CF (1980) Numerical prediction of convectively driven mesoscale pressure systems. Part I: convective parameterization. J Atmos Sci 37:1722–1733

Gallée H, Moufouma-Okia W, Bechtold P, Brasseur O, Dupays I (2004) A high-resolution simulation of a West African rainy season using a regional climate model. J Geophys Res 109:D05108. doi:10.1029/2003JD004020

Gao X, Zhang D, Chen Z, Pal J, Giorgi F (2007) Land use effects on climate in China as simulated by a regional climate model. Science in China. Ser D Earth Sci 50(4):620–628

Giorgi F, Mearns LO (1999) Introduction to special section: regional climate modelling revisited. J Geophys Res 104:6335–6352

Giorgi F, Marinucci MR, Bates GT (1993a) Development of a second-generation regional climate model (RegCM2). Part I: boundary-layer and radiative transfer processes. Mon Weather Rev 121(10):2794–2813

Giorgi F, Marinucci MR, Bates GT, Canio GD (1993b) Development of a second-generation regional climate model (RegCM2). Part II: convective processes and assimilation of lateral boundary conditions. Mon Weather Rev 121:2814–2832

Giorgi F, Brodeur CS, Bates GT (1994) Regional climate change scenarios over the United States produced with a nested regional climate model. J Clim 7:375–399

Giorgi F, Mearns LO, Shields C, McDaniel L (1998) Regional nested model simulations of present day and 2× CO_2 climate over the Central Plains of the US. Clim Change 40:457–493

Giorgi F, BI X, Pal J (2004) Mean, interannual variability and trends in a regional climate experiment over Europe. II: future climate (2070–2100). Clim Dyn 23(7–8):839–858

Giorgi F, Diffenbaugh NS, Gao XJ, Coppola E, Dash SK, Frumento O, Rauscher SA, Remedio A, Sanda IS, Steiner A, Sylla B, Zakey AS (2008) The regional climate change hyper-matrix framework. Eos 89(45):445–456

Giorgi F, Coln J, Ghassem A (2009) addressing climate information needs at the regional level. The CORDEX framework. WMO Bulletin, July 2009 issue

Grell GA, Dudhia J, Stauffer DR (1994) Description of the fifth generation Penn State/NCAR mesoscale model (MM5). Technical note NCAR/TN-398+STR, p 121

Grist JP, Nicholson SE (2001) A study of the dynamic factors influencing the rainfall variability in the West African Sahel. J Clim 14:1337–1359

Herman A, Kumar V, Arkin P, Kousky J (1997) Objectively determined 10-day African rainfall estimates created for famine early warning systems. Int J Remote Sens 18:2147–2159

Holtslag AAM, De Bruin EIF, Pan HL (1990) A high resolution air mass transformation model for short-range weather forecasting. Mon Weather Rev 118:1561–1575

Hudson DA, Jones R (2002) Regional Climate Model simulations of present—day and future climates of southern Africa. Technical note 39, Hadley Centre for Climate Prediction and Research, Met Off Bracknell, England

Im ES, Kwon WT, Ahn JB, Giorgi F (2007) Multi-decadal scenario simulation over Korea using a one-way double-nested regional climate model system. Part I: recent climate simulation (1971–2000). Clim Dyn 28(75):9–780

Im ES, Ahn JB, Kwon WT, Giorgi F (2008) Multi-decadal scenario simulation over Korea using a one-way double-nested regional climate model system. Part II: future climate projection (2021–2050). Clim Dyn 30(23):9–254

Indeje M, Semazzi FHM, Ogallo LJ (2000) ENSO signals in East African rainfall seasons. Int J Climatol 20:19–46

Janicot S, Moron V, Fontaine B (1996) Sahel drought and ENSO dynamics. Geophys Res Lett 23:515–518

Jenkins GS, Gaye AT, Sylla MB (2005) Late 20th century attribution of drying trends in the Sahel from the regional climate model (RegCM3). Geophys Res Lett 32:L22705

Jones RG, Murphy JM, Noguer M (1995) Simulation of climate change over Europe using a nested regional climate model I: assessment of control climate, including sensitivity to location of lateral boundary conditions. Q J R Meteorol Soc 121:1413–1449

Jung G, Kunstmann H (2007) High-resolution regional climate modeling for the Volta region of West Africa. J Geophys Res 112:D23108. doi:10.1029/2006JD007951

Jury MR, Pathack CJ, Rautenbach WD, Heerden JV (1996) Drought over southern Africa and Indian Ocean SST: statistical correlations and GCM results. Glob Ocean Atmos Syst 4:47–63

Kiehl JT, Hack JJ, Bonan GB, Boville BA, Briegleb BP, Williamson DL, Rasch PJ (1996) Description of the NCAR Community Climate Model (CCM3), Technical Report TN-420+STR, NCAR, Boulder, p 152

Konare A, Zakey AS, Solmon F, Giorgi F, Rauscher S, Ibrah S, Bi X (2008) A regional climate modeling study of the effect of desert dust on the West African monsoon. J Geophys Res 113:D12206. doi:10.1029/2007JD009322

Leung LR, Qian Y, Bian X, Washington WM, Han J, Roads JO (2004) Mid-century ensemble regional climate change scenarios for the western United States. Clim Change 62:75–113

Mathon V, Laurent H (2001) Life cycle of Sahelian mesoscale convective cloud systems. Q J R Meteorol Soc 127:377–406

McGregor JL, Katzfey JJ, Nguyen KC (1998) Fine resolution simulations of climate change for Southeast Asia. Final report for a Research Project commissioned by Southeast Asian Regional Committee for START (SARCS), Aspendale, Vic., CSIRO Atmospheric Research VI, pp 15–35

Mearns LO, Giorgi F, McDaniel L, Shields C (1995) Analysis of daily precipitation variability in a nested regional climate model: comparison with observations and 2× CO_2 results. Glob Planet Change 10:55–78

Mitchell TD, Carter TR, Jones PD, Hulme M, New M (2004) A Comprehensive Set of High-resolution grids of monthly climate for Europe and the globe: the observed record (1901–2000) and 16 scenarios (2001–2100). Tyndall Centre for Climate Change Research, Norwich, Working Paper 55

Mohr KI, Thorncroft CD (2006) Intense convective systems in West Africa and their relationship to the African easterly jet. Quat J Meteorol Soc 132:163–176

Mutemi JN, Ogallo LA, Krishnamurti TN, Mishra AK, Vijaya KTSV (2007) Multimodel based superensemble forecasts for short and medium range NWP over various regions of Africa. Meteorol Atmos Phys 95:87–113

Mwafulirwa ND (1999) Climate variability and predictability in tropical southern Africa with focus on dry spells over Malawi. M.Sc. thesis, University of Zululand

Noguer M, Jones RG, Murphy JM (1998) Sources of systematic errors in the climatology of a nested regional climate model (RCM) over Europe. Clim Dyn 14:691–712

Paeth H, Born K, Podzun R, Jacob D (2005) Regional dynamical downscaling over West Africa: model evaluation and comparison of wet and dry years. Meteorol Z 14(3):349–367

Pal JS, Eltahir EAB (2003) A feedback mechanism between soil moisture distribution and storm tracks. Q J R Meteorol Soc 129:2279–2297

Pal JS, Small EE, Eltahir EAB (2000) Simulation of regional-scale water and energy budgets: representation of subgrid cloud and precipitation processes within RegCM. J Geophys Res 105:29579–29594

Pal J, Giorgi F, Bi X (2004) Consistency of recent European summer precipitation trends and extremes with future regional climate projections. Geophys Res lett 31(L13202). doi:10.1029/2004GL019836

Pal JS, Giorgi F, Bi X, Elguindi N, Solomon F, Gao X, Francisco R, Zakey A, Winter J, Ashfaq M, Syed F, Bell JL, Diffanbaugh NS, Kamacharya J, Konare A, Martinez D, da Rocha RP, Sloan LC, Steiner A (2007) The ICTP RegCM3 and RegCNET: regional climate modeling for the developing world. Bull Am Meteorol Soc 88:1395–1409

Rauscher SA, Seth A, Qian JH, Camargo SJ (2006) Domain choice in an experimental nested modeling prediction system for South America. Theor Appl Climatol 86:229–246. doi:10.1007/s00704-006-0206-z

Reason CJC, Rouault M (2005) Links between the Antarctic Oscillation and winter rainfall over western South Africa. Geophys Res lett 32. doi:10.1029/2005GL022419

Segele ZT, Leslie LM, Lamb PJ (2008) Evaluation and adaptation of a regional climate model for the Horn of Africa: rainfall climatology and interannual variability. Inter J Climatol. doi:10.1002/joc.1681

Seth A, Rauscher SA, Carmago SJ, Qian JH, Pal J (2006) RegCM3 regional climatologies for South America using reanalysis and ECHAM global model driving fields. Clim Dyn 28:461–480. doi:10.1007/s00382-006-0191-z

Simmons AS, Uppala DD, Kobayashi S (2007) ERA-interim: new ECMWF reanalysis products from 1989 onwards. ECMWF Newsl 110:29–35

Steiner AL, Pal JS, Rauscher SA, Bell JL, Diffenbaugh NS, Boone A, Sloan LC, Giorgi F (2009) Land surface coupling in regional climate simulations of the West African monsoon. Clim Dyn. doi:10.1007/s00382-009-0543-6

Sun L, Semazzi FHM, Giorgi F, Ogallo LA (1999a) Application of the NCAR regional climate model to eastern Africa. Part I: simulation of the short rains of 1988. J Geophys Res 104:6529–6548

Sun L, Semazzi FHM, Giorgi F, Ogallo LA (1999b) Application of the NCAR regional climate model to eastern Africa. Part II: simulation of interannual variability of short rains. J Geophys Res 104:6549–6562

Sylla MB, Gaye AT, Pal JS, Jenkins GS, Bi XQ (2009) High resolution simulations of West Africa climate using Regional Climate Model (RegCM3) with different lateral boundary conditions. Theor Appl Climatol. doi:10.1007/s00704-009-0110-4

Tadross MA, Gutowski WJ, Hewitson BC, Jack C, New M (2006) MM5 simulations of interannual change and the diurnal cycle of southern African regional climate. Theor Appl Climatol 86:63–80

Thorncroft CD, Blackburn M (1999) Maintenance of the African Easterly Jet. Q J R Meteorol Soc 125:763–786

Trenberth KE, Stepaniak DP, Hurrell JW (2001) Quality of reanalyses in the tropics. J Clim 14:1499–1510

Uppala S, Dee D, Kobayashi S, Berrisford P, Simmons A (2008) Towards a climate data assimilation system: status update of ERA-interim. ECMWF Newsl 115:12–18

Vizy E, Cook K (2002) Development and application of a mesoscale climate model for the tropics: influence of sea surface temperature anomalies on the West African monsoon. J Geophys Res 107 D(3). doi:10.1029/2001JD000686

Wang Y, Leung LR, McGregor JL, Lee DK, Wang WC, Ding Y, Kimura F (2004) Regional climate modeling: progress, challenges and prospects. J Meteorol Soc Jpn 82:1599–1628

Zeng X, Zhao M, Dickinson RE (1998) Intercomparison of bulk aerodynamic algorithms for the computation of sea surface fluxes using TOGA COARE and TAO data. J Clim 11:2628–2644